Effective Control of Superconducting Qubit Systems via Heterodyne Experimental Setups: Mechanisms, Noise Considerations, and Performance Factors

Denys Derlian C. Brito[1], André J. C. Chaves[1]
[1]Instituto Tecnológico de Aeronáutica, São José dos Campos/São Paulo — Brasil

***Abstract*— The development of scalable, fault-tolerant quantum computers hinges on the ability to execute quantum logic operations with exceptionally high fidelity. For superconducting circuits, a leading platform for quantum information processing, this necessitates precise control over qubit states using engineered microwave pulses. This report provides a comprehensive framework for understanding the effective control of superconducting qubit systems through heterodyne experimental setups. We begin by establishing the theoretical foundations of qubit-resonator interactions, tracing the progression from the fundamental Rabi model to the practical dispersive Hamiltonian. A model of the heterodyne signal generation and delivery chain is presented, connecting the classical control electronics to the quantum dynamics of the qubit. We systematically categorize and quantify noise sources originating from the control electronics, the quantum system's environment, and system-level interactions. Finally, we discuss advanced strategies for noise mitigation, including optimal control pulse shaping and dynamical decoupling, and provide practical guidelines for the design, calibration, and operation of high-performance qubit control systems.**

***Keywords*— Quantum Hardware, Superconducting Qubits, Quantum Control, Microwave Pulse Engineering, Circuit Quantum Electrodynamics.**

I. Introduction

The realization of fault-tolerant quantum computation hinges on implementing quantum logic gates with error rates below the threshold required by quantum error correction codes [1], [2]. For superconducting circuits, a leading quantum platform, this translates to achieving single-operation fidelities well above 99.9% [3]. As qubit coherence improves, the classical electronics used for control and readout are increasingly becoming the primary performance bottleneck [3], [4].

The pursuit of high-fidelity qubit control is not solely an academic endeavor; it is a critical enabler for a new generation of defense and military technologies [5]. The computational power promised by fault-tolerant quantum computers could revolutionize military operations [5], [6], from breaking complex cryptographic codes to solving intractable optimization problems in logistics, resource allocation, and mission planning [6].

Superconducting qubits operate at microwave frequencies, and their states are manipulated and measured using microwave signals generated by room-temperature electronics [3], [7]. The standard method for generating these precise control pulses is heterodyne up-conversion using in-phase and quadrature (IQ) mixers [8], [9]. This technique provides full control over the pulse's amplitude, phase, and frequency. However, the control hardware itself is a major source of noise and a significant challenge for scalability. Increasing the number of qubits requires more control lines, which adds thermal load to the cryogenic system, increases signal crosstalk, and complicates the calibration of analog components that are prone to drift [10]–[12].

This report provides a unified framework connecting the classical control hardware, quantum dynamics, and the noise sources that limit performance in these systems. This report is structured as follows. Sec. II reviews the principles of qubit control and measurement within the Circuit Quantum Electrodynamics (cQED) architecture. Sec. III introduces the theoretical framework, including the system's Hamiltonian and open system dynamics. We then detail the heterodyne signal processing for control and readout in Sec. IV. The experimental apparatus is modeled in Sec. V, followed by an analysis of noise sources in Sec. VI. Sec. VII discusses mitigation strategies and the future outlook for scalable control hardware, before our conclusion in Sec. VIII.

II. Background: Principles of Qubit Control and Signal Generation

In cQED, a superconducting qubit is coupled to a microwave resonator [13], [14]. This resonator serves to protect the qubit, mediate interactions, and perform readout [14], [15]. The most common qubit type is the *transmon* [16], favored for its long coherence times but limited by low anharmonicity, which can cause leakage to non-computational states [17], [18]. Other designs, like the *fluxonium*, offer higher anharmonicity and improved noise protection [1], [4]. Qubit control and readout are achieved by generating microwave pulses using heterodyne techniques. An Arbitrary Waveform Generator (AWG) produces low-frequency in-phase $I(t)$ and quadrature $Q(t)$ waveforms, which are then up-converted to the qubit frequency using an IQ mixer and a Local Oscillator (LO) [14], [19]–[21]. This allows for the synthesis of pulses with arbitrary amplitude and phase, enabling universal quantum gates. The same principle is used in reverse for readout, where faint microwave signals from the qubit are down-converted to be digitized and analyzed [9], [22].

The same heterodyne principle that is used to generate control pulses is also employed for qubit state measurement.

Denys Derlian C. Brito, derlian@ita.com; André J. C. Chaves, andrej6@gmail.com.

In the cQED architecture, qubit readout is typically performed dispersively: the resonance frequency of the coupled resonator is shifted by a small amount that depends on the state of the qubit [14]. To measure this shift, a microwave probe tone is sent to the resonator, and the transmitted or reflected signal is analyzed.

This faint signal, carrying the quantum state information in its amplitude and phase, must be amplified and brought back to a frequency range where it can be digitized. This is achieved through heterodyne down-conversion [14], [19], [21]. The signal from the cryostat is first amplified by a chain of cryogenic and room-temperature amplifiers and then fed into a mixer. There, it is mixed with an LO, often the same one used for generating the probe tone to ensure phase coherence. This process shifts the signal from the multi-GHz microwave domain down to a low intermediate frequency (IF) or directly to DC (a homodyne measurement). The resulting I and Q components of the signal are then digitized by a high-speed analog-to-digital converter (ADC) and processed in software to discriminate between the different qubit states [8], [14], [19]. Thus, the heterodyne setup serves a dual role, enabling both the "writing" of quantum information via pulse synthesis and the "reading" of it via signal demodulation.

III. Theoretical Framework for Qubit-Control Interaction

The interaction between a qubit and a resonator is fundamentally described by the Quantum Rabi model [23]. In most experiments, where the coupling g is much weaker than the qubit and resonator frequencies (ω_q, ω_r), the Rotating Wave Approximation (RWA) is applied, simplifying the system to the well-known Jaynes-Cummings Model [24]–[27]. For readout and many gate operations, the system is operated in the dispersive limit, where the detuning $\Delta = \omega_q - \omega_r$ is much larger than the coupling, $|\Delta| \gg g$ [14]. In this regime, the effective Hamiltonian becomes:

$$H_{\text{disp}} \approx \hbar\left(\omega_r + \chi\hat{\sigma}_z\right)\hat{a}^\dagger\hat{a} + \frac{\hbar}{2}\left(\omega_q + \chi\right)\hat{\sigma}_z, \tag{1}$$

the key parameter is the dispersive shift, $\chi \approx -g^2/\Delta$, which describes how the resonator frequency is shifted based on the qubit state ($\hat{\sigma}_z$). This state-dependent shift is the physical basis for dispersive readout.

An external microwave drive, used to perform quantum gates, is modeled as a time-dependent term in the Hamiltonian. In the rotating frame, this simplifies to a rotation operator whose Rabi frequency $\Omega(t)$ and phase $\phi(t)$ are directly controlled by the $I(t)$ and $Q(t)$ waveforms from the AWG [28]–[30]. Real quantum systems are open and interact with their environment, leading to decoherence. This is modeled using the Lindblad master equation, which describes the evolution of the system's density matrix ρ [31]:

$$\frac{d\rho}{dt} = -\frac{i}{\hbar}[H,\rho] + \sum_k \left(L_k\rho L_k^\dagger - \frac{1}{2}\{L_k^\dagger L_k, \rho\}\right), \tag{2}$$

here, the Hamiltonian H describes coherent evolution, while the Lindblad "jump" operators L_k model incoherent processes like energy relaxation (related to the relaxation time of the system - T_1) and dephasing (related to the phase decoherence time - T_2). For tracking a single quantum system under continuous measurement, Quantum Trajectory Theory (QTT) is used, which models the stochastic evolution of the state based on the measurement record [14], [15], [25].

IV. Heterodyne Signal Processing for Qubit Control and Readout

High-fidelity control and measurement of superconducting qubits are dependent on the precise generation and analysis of microwave signals. The experimental architecture, as depicted in Fig. 2, employs heterodyne techniques for both frequency up-conversion of control pulses and down-conversion of readout signals. This method allows for the use of high-precision, lower-frequency AWGs to define the complex envelope of microwave signals operating in the gigahertz regime.

A. Single-Sideband Up-conversion for Qubit Control

To execute quantum gates, shaped microwave pulses must be delivered to the qubit at its transition frequency, ω_q, which typically lies in the 3-6 GHz range. These pulses require precise control over their amplitude and phase envelope. This is achieved by synthesizing the pulse at a lower IF and then up-converting it using an IQ mixer, a process known as Single-Sideband (SSB) modulation [32], [33].

The desired pulse envelope is defined by a time-dependent amplitude $A(t)$ and phase $\phi(t)$. An AWG generates two corresponding baseband signals, the in-phase I and quadrature Q components:

$$I(t) = A(t)\cos(\phi(t)), \tag{3}$$

$$Q(t) = A(t)\sin(\phi(t)), \tag{4}$$

these baseband signals are then mixed with a continuous-wave LO signal, $V_{LO}(t) = \cos(\omega_{LO}t)$. The IQ mixer functions as a Hartley modulator, multiplying the $I(t)$ and $Q(t)$ signals with phase-quadrature components of the LO and summing them [14]. To generate an upper-sideband signal at the target qubit frequency $\omega_q = \omega_{LO} + \omega_{IF}$, the baseband signals are first modulated at an intermediate frequency ω_{IF} and then mixed. The mathematical operation of the mixer can be expressed as:

$$V_{\text{out}}(t) = A(t)\cos((\omega_{LO} + \omega_{IF})t + \phi(t)). \tag{5}$$

The result is a microwave pulse at the desired qubit frequency $\omega_q = \omega_{LO} + \omega_{IF}$, with its envelope precisely defined by the AWG-generated signals. The lower sideband at $\omega_{LO} - \omega_{IF}$ is suppressed by the quadrature architecture of the mixer. This technique provides complete control over the pulse's amplitude and phase, which is essential for implementing high-fidelity quantum gates.

B. Heterodyne Down-conversion and Signal Demodulation

Qubit state measurement is performed dispersively by probing a coupled readout resonator. The resonator's frequency is shifted by $\pm\chi$ depending on the qubit state, $|0\rangle$ or $|1\rangle$ [14]. A probe tone at frequency ω_p is directed to the resonator, and the reflected signal, $V_{\text{in}}(t)$, acquires a state-dependent amplitude A_r and phase ϕ_r. After cryogenic and room-temperature amplification, this weak microwave signal must be demodulated to extract this information.

Heterodyne detection is used to down-convert the amplified signal from the probe frequency ω_p to a digitizable intermediate frequency $\omega_{IF} = |\omega_p - \omega_{LO}|$. The incoming signal,

$V_{\text{in}}(t) = A_r \cos(\omega_p t + \phi_r)$, is fed into an IQ mixer along with an LO signal at ω_{LO}. The mixer produces two outputs, which after low-pass filtering to remove sum-frequency components, are:

$$V_I(t) \propto A_r \cos((\omega_p - \omega_{LO})t + \phi_r) = A_r \cos(\omega_{IF} t + \phi_r), \tag{6}$$

$$V_Q(t) \propto A_r \sin((\omega_p - \omega_{LO})t + \phi_r) = A_r \sin(\omega_{IF} t + \phi_r). \tag{7}$$

These two orthogonal signals at ω_{IF} contain the amplitude and phase information of the original high-frequency signal. An ADC then digitizes them. To recover the baseband signal, a digital demodulation is performed. The digitized signals are treated as a complex value, $S(t) = V_I(t) + iV_Q(t)$, which is then multiplied by a complex digital reference oscillator:

$$S_{\text{baseband}}(t) = S(t)e^{-i\omega_{IF}t} \propto A_r e^{i(\omega_{IF}t+\phi_r)} e^{-i\omega_{IF}t} = A_r e^{i\phi_r}. \tag{8}$$

To improve the signal-to-noise ratio, this time-independent complex value is integrated over the measurement duration T_{meas}:

$$I + iQ = \int_0^{T_{\text{meas}}} S_{\text{baseband}}(t)dt, \tag{9}$$

this process yields a single complex point (I, Q) in the complex plane for each measurement shot.

C. State Discrimination in the IQ Plane

A single measurement shot produces one (I, Q) point. Due to system noise and quantum projection noise, this process is repeated thousands of times for known initial states ($|0\rangle$ and $|1\rangle$) to build statistical distributions. When plotted, these points form two distinct clusters, or "blobs", in the IQ plane, which are often well-approximated by two-dimensional Gaussian distributions [14], [34]. The separation between the centers of the $|0\rangle$ and $|1\rangle$ state clusters is a direct consequence of the qubit-state-dependent resonator response.

Qubit state discrimination is the task of classifying a subsequent measurement of an unknown state based on its resulting (I, Q) coordinate. This is achieved by establishing a decision boundary in the IQ plane that optimally separates the two calibrated clusters. In the simplest case, a linear discriminator — a line that bisects the vector connecting the two cluster centroids — is used to partition the plane into two regions corresponding to the $|0\rangle$ and $|1\rangle$ states, as seen in Fig. 1. The fidelity of the measurement is ultimately determined by the degree of overlap between the two statistical distributions; less overlap corresponds to higher assignment fidelity.

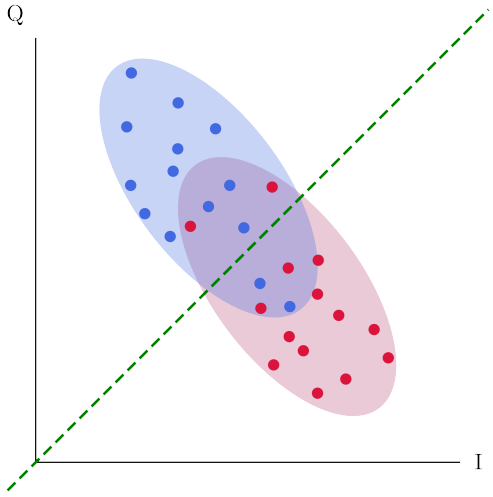

Fig. 1: Illustration of single-qubit state discrimination using heterodyne detection in the IQ plane. Each point represents a single-shot measurement outcome, where the qubit was prepared in either the ground state (blue) or the excited state (red). The dashed green line indicates a linear decision boundary (discriminant) used for state classification. The shaded ellipses depict Gaussian mixture model fits to the measurement distributions for each state, capturing their statistical spread due to noise and imperfections in the measurement chain.

V. Modeling the Experimental Control Apparatus

This section presents a standard experimental control apparatus for heterodyne signal processing for qubit control and readout. An illustrative schema can be visualized in Fig. 2.

A. Detailed Signal Path: From AWG to Qubit

The control signal path begins at room temperature, where an AWG generates baseband I/Q waveforms that are up-converted by an IQ mixer driven by an LO. The resulting microwave pulse is then sent into the dilution refrigerator through coaxial cables. Inside the cryostat, the signal is heavily attenuated at multiple temperature stages (e.g., 4 K, 100 mK, 10 mK) to reduce its power to the single-photon level and, crucially, to thermalize the line, preventing room-temperature thermal noise from reaching the qubit [19]. The entire chain can introduce distortions that must be pre-compensated in the AWG waveform to ensure high-fidelity operations [19], [29].

B. The Cryogenic Environment: Scaling Challenges

The cryogenic environment imposes significant constraints on scalability. Each control line introduces a thermal load into the cryostat. For a large-scale processor with thousands of qubits, the cumulative heat load from the necessary wiring would overwhelm the cooling power of dilution refrigerators [8]. Furthermore, readout requires bulky, magnetic, non-reciprocal components like circulators and isolators to protect the qubit from amplifier noise. The size and thermal mass of these components for many qubits present a formidable engineering challenge, motivating the development of more integrated control solutions [8], [35].

VI. Analysis of Noise Sources and Impact on Control Fidelity

High-fidelity quantum control is a constant battle against noise from numerous sources. These can be broadly categorized into noise originating from the classical control electronics and noise inherent to the quantum system and its environment. A qualitative overview of these sources is presented below, and the qualitative results are compiled in Table I.

To understand the relative importance of these varied noise sources, it is instructive to compile them into a unified error budget. The total infidelity of a quantum gate can be

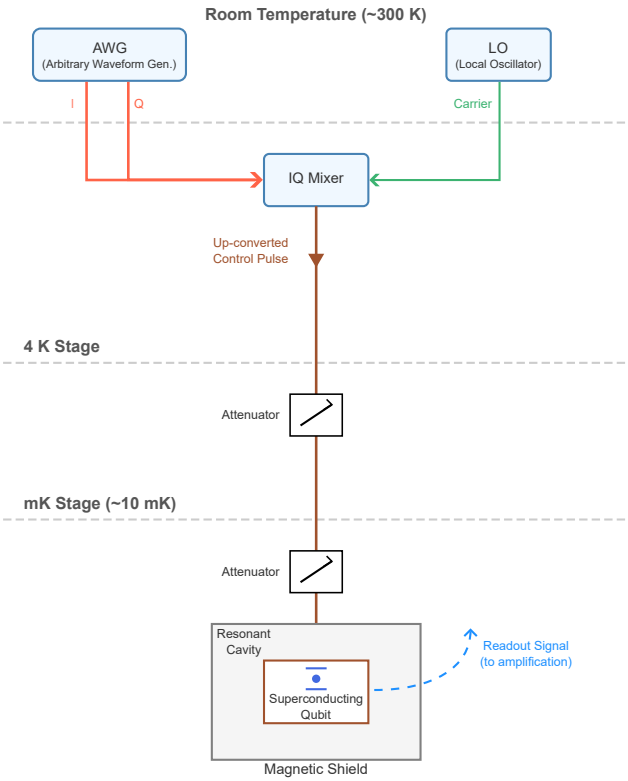

(a) Control signal generation and delivery chain. Microwave control pulses are generated at room temperature by mixing IF signals from an AWG with a LO tone using an IQ mixer. The up-converted pulses are attenuated at cryogenic stages before reaching the superconducting qubit housed inside a resonant cavity at millikelvin temperatures.

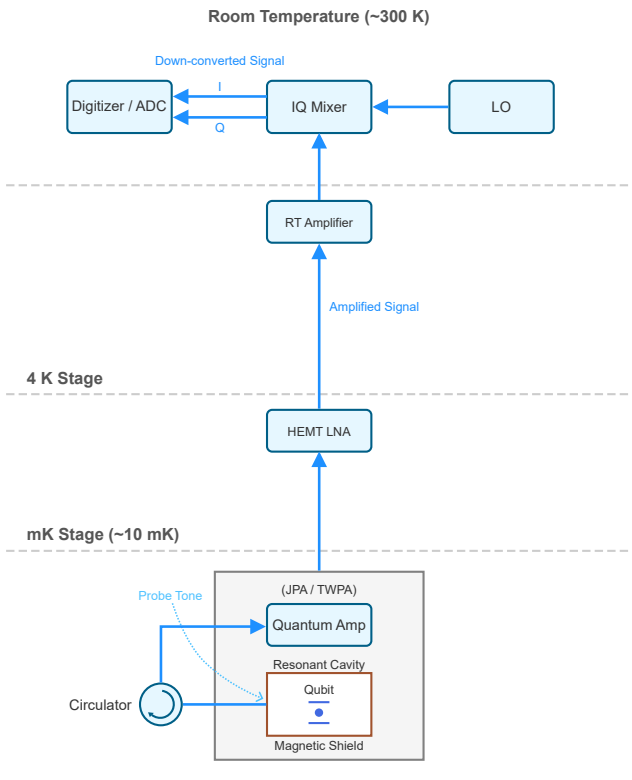

(b) Measurement and readout chain. The qubit state-dependent signal reflects from the cavity and passes through a circulator to a quantum-limited amplifier (e.g., JPA or TWPA) at the mK stage. It is further amplified by a HEMT amplifier at 4 K and room-temperature amplifiers before being down-converted by an IQ mixer and digitized by an ADC.

Fig. 2: Schematic overview of the control and readout architecture for a superconducting qubit experiment. (2a) The control chain delivering shaped microwave pulses to drive qubit rotations. (2b) The readout chain for dispersively measuring the qubit state through reflected microwave signals, including cryogenic and room-temperature amplification and heterodyne down-conversion.

approximated as the sum of probabilities of different error events. This provides a diagnostic framework for identifying and targeting the dominant performance limitations in a given experimental setup.

VII. Discussion: Synthesis and Practical Implications

A. Critical Parameters and Mitigation Strategies

The pursuit of high-fidelity quantum computation is co-limited by the quality of the quantum hardware and the precision of the classical control electronics. For a perfect qubit, fidelity is limited by control signal stability (LO phase noise, amplitude noise, mixer calibration) [12], [19], [29]. For perfect electronics, fidelity is limited by the qubit's intrinsic material-based decoherence (TLS, 1/f noise) [18], [36]. As systems scale, crosstalk becomes a dominant bottleneck [19].

Advanced techniques are used to combat these noise sources.

- **Optimal Control and Pulse Shaping:** Instead of simple pulses, advanced waveforms are designed to be robust against specific errors. *Derivative Removal by Adiabatic Gate* (DRAG) is an analytical technique that modifies pulse shapes to suppress leakage to non-computational states, a key issue for transmons [37], [38]. *Quantum Optimal Control Theory* uses numerical algorithms to discover high-fidelity pulse shapes, but its performance depends on an accurate model of the system [39], [40]. Modern approaches lead into the usage of Machine-Learning-based techniques [41]–[44].
- **Dynamical Decoupling (DD):** This technique mitigates low-frequency noise by applying a sequence of refocusing π-pulses (e.g., Hahn echo, CPMG, XY4) during idle periods [45], [46]. This averages out the effect of slow noise fluctuations. Advanced DD sequences can also be designed to suppress crosstalk between qubits, a critical tool for multi-qubit processors [47], [48].

B. Practical Guidelines and Future Outlook

Achieving high fidelity requires a data-driven, full-stack approach. This begins with thorough system characterization, including in-situ mixer calibration using the qubit as a sensor [21] and noise spectroscopy to identify dominant error sources [49]. The choice of mitigation strategy — DD for low-frequency noise, DRAG for leakage — should be based on this diagnosis.

The limitations of traditional analog heterodyne systems (calibration drift, size, thermal load) are driving a shift towards integrated, digital-first control hardware [50]. RF System-on-Chip (RFSoC) platforms, which integrate DACs, ADCs, and FPGAs, represent the next generation [51]–[53]. By

TABELA I: Qualitative Summary of Key Noise Sources Affecting Superconducting Qubit Control Fidelity

Noise Source	Physical Origin	Impact on Qubit	Mitigation Strategy
LO Phase Noise	Frequency instability in local oscillator.	Introduces qubit dephasing and limits gate speed.	Use ultra-low phase noise oscillators; apply dynamical decoupling sequences.
LO Amplitude Noise	Fluctuations in LO power or drive chain gain.	Causes over-rotation or under-rotation in gate operations.	Power stabilization; pulse shaping at amplitude sweet spots.
IQ Mixer Imbalance	Gain and phase mismatch between I and Q channels.	Leads to unwanted frequency components and off-resonant driving.	Regular mixer calibration; apply digital predistortion.
LO Leakage	Imperfect isolation in IQ mixer.	Adds unintended continuous drive tone, inducing Stark shifts and state errors.	DC offset correction; use high-isolation mixers.
Mixer Nonlinearities	Non-ideal mixer diode behavior.	Generates spurious harmonics and sidebands, risking leakage to non-computational states.	Apply low-pass filtering; use highly linear mixers or DDS-based control.
ZZ Crosstalk	Static coupling between qubits due to chip layout.	Creates state-dependent frequency shifts on neighboring qubits, especially during parallel gates.	Implement tunable couplers; optimize frequency allocation; use echo sequences.
Microwave Crosstalk	Electromagnetic leakage between control lines.	Causes unintentional driving of nearby qubits.	Improve chip shielding; design crosstalk cancellation pulses.
Dielectric Loss (TLS)	Atomic defects in materials near the qubit.	Reduces T_1 and T_2, degrading intrinsic coherence.	Fabrication improvements; surface treatments; use of low-loss dielectrics.
1/f Flux and Charge Noise	Slow fluctuations in magnetic flux or charge.	Causes low-frequency dephasing and frequency drift.	Operate at sweet spots; apply dynamical decoupling.
Quasiparticle Tunneling	Broken Cooper pairs acting as dissipative channels.	Limits T_1, especially for small junction devices.	Engineer quasiparticle traps; improve shielding from stray radiation.
Readout-Induced Noise	Residual photons or backaction from the measurement chain.	Causes dephasing post-measurement, limiting coherence after readout.	Optimize resonator depletion time; use Purcell or nonlinear filters.

digitizing signal generation and processing, these systems promise higher stability, reduced complexity, and the low-latency feedback essential for quantum error correction.

VIII. Conclusion

The effective control of superconducting qubits via heterodyne setups is a complex challenge at the intersection of quantum theory, microwave engineering, and materials science. Our analysis reveals a landscape of noise sources, from the classical control electronics to the quantum device itself, that collectively limit gate fidelity. While traditional analog systems have been instrumental, their scalability and stability limitations are clear. The future of high-fidelity control lies in integrated, digital-dominant architectures like RFSoCs, combined with advanced noise mitigation protocols such as optimal control and dynamical decoupling. This integrated approach is essential for overcoming the control challenges on the path to building large-scale, fault-tolerant quantum computers.

References

[1] H. Yang and N. Y. Kim, "Material-inherent noise sources in quantum information architecture," *Materials*, vol. 16, no. 7, 2023. [Online]. Available: https://www.mdpi.com/1996-1944/16/7/2561

[2] F. Pastawski and B. Yoshida, "Fault-tolerant logical gates in quantum error-correcting codes," *Physical Review A*, vol. 91, 2014. [Online]. Available: https://api.semanticscholar.org/CorpusID:15105507

[3] J. van Dijk, E. Kawakami, R. Schouten, M. Veldhorst, L. Vandersypen, M. Babaie, E. Charbon, and F. Sebastiano, "Impact of classical control electronics on qubit fidelity," *Phys. Rev. Appl.*, vol. 12, p. 044054, Oct 2019. [Online]. Available: https://link.aps.org/doi/10.1103/PhysRevApplied.12.044054

[4] D. A. Rower, L. Ding, H. Zhang, M. Hays, J. An, P. M. Harrington, I. T. Rosen, J. M. Gertler, T. M. Hazard, B. M. Niedzielski, M. E. Schwartz, S. Gustavsson, K. Serniak, J. A. Grover, and W. D. Oliver, "Suppressing counter-rotating errors for fast single-qubit gates with fluxonium," *PRX Quantum*, vol. 5, p. 040342, Dec 2024. [Online]. Available: https://link.aps.org/doi/10.1103/PRXQuantum.5.040342

[5] D. D. Carvalho Brito, R. Pires Ferreira, and A. J. Chaves, "Perspectivas globais militares sobre tecnologias quânticas," *Spectrum - The Journal of Operational Applications in Defense Areas*, vol. 24, no. 1, p. 54–60, set. 2023. [Online]. Available: https://spectrum.ita.br/index.php/spectrum/article/view/389

[6] M. Krelina, "Quantum technology for military applications," *EPJ Quantum Technology*, vol. 8, no. 1, Nov. 2021. [Online]. Available: http://dx.doi.org/10.1140/epjqt/s40507-021-00113-y

[7] M. C. Smith, A. D. Leu, K. Miyanishi, M. F. Gely, and D. M. Lucas, "Single-qubit gates with errors at the 10^{-7} level," *Phys. Rev. Lett.*, vol. 134, p. 230601, Jun 2025. [Online]. Available: https://link.aps.org/doi/10.1103/42w2-6ccy

[8] M. Kjaergaard, M. E. Schwartz, J. Braumüller, P. Krantz, J. I.-J. Wang, S. Gustavsson, and W. D. Oliver, "Superconducting qubits: Current state of play," *Annual Review of Condensed Matter Physics*, vol. 11, no. Volume 11, 2020, pp. 369–395, 2020. [Online]. Available: https://www.annualreviews.org/content/journals/10.1146/annurev-conmatphys-031119-050605

[9] A. Anferov, F. Wan, S. P. Harvey, J. Simon, and D. I. Schuster, "Millimeter-wave superconducting qubit," *PRX Quantum*, vol. 6, p. 020336, May 2025. [Online]. Available: https://link.aps.org/doi/10.1103/PRXQuantum.6.020336

[10] G. Zhu, D. G. Ferguson, V. E. Manucharyan, and J. Koch, "Circuit qed with fluxonium qubits: Theory of the dispersive regime," *Phys. Rev. B*, vol. 87, p. 024510, Jan 2013. [Online]. Available: https://link.aps.org/doi/10.1103/PhysRevB.87.024510

[11] L. Stefanazzi, K. Treptow, N. Wilcer, C. Stoughton, C. Bradford, S. Uemura, S. Zorzetti, S. Montella, G. Cancelo, S. Sussman, A. Houck, S. Saxena, H. Arnaldi, A. Agrawal, H. Zhang, C. Ding, and D. I. Schuster, "The qick (quantum instrumentation control kit): Readout and control for qubits and detectors," *Review of Scientific Instruments*, vol. 93, no. 4, Apr. 2022. [Online]. Available: http://dx.doi.org/10.1063/5.0076249

[12] Y. Y. Gao, M. A. Rol, S. Touzard, and C. Wang, "Practical guide for building superconducting quantum devices," *PRX Quantum*, vol. 2, p. 040202, Nov 2021. [Online]. Available: https://link.aps.org/doi/10.1103/PRXQuantum.2.040202

[13] C. J. Howington, "Digital readout and control of a superconducting qubit," PhD Dissertation, Syracuse University, December 2019, open Access. Available at https://surface.syr.edu/etd/1121.

[14] P. Krantz, M. Kjaergaard, F. Yan, T. P. Orlando, S. Gustavsson, and W. D. Oliver, "A quantum engineer's guide to superconducting qubits," *Applied Physics Reviews*, vol. 6, no. 2, Jun. 2019. [Online]. Available: http://dx.doi.org/10.1063/1.5089550

[15] A. Blais, A. L. Grimsmo, S. M. Girvin, and A. Wallraff, "Circuit quantum electrodynamics," *Rev. Mod. Phys.*, vol. 93, p. 025005, May 2021. [Online]. Available: https://link.aps.org/doi/10.1103/RevModPhys.93.025005

[16] J. Koch, T. M. Yu, J. Gambetta, A. A. Houck, D. I. Schuster, J. Majer, A. Blais, M. H. Devoret, S. M. Girvin, and R. J. Schoelkopf, "Charge-insensitive qubit design derived from the cooper pair box," *Phys. Rev. A*, vol. 76, p. 042319, Oct 2007. [Online]. Available: https://link.aps.org/doi/10.1103/PhysRevA.76.042319

[17] A. A. Houck, J. Koch, M. H. Devoret, S. M. Girvin, and R. J. Schoelkopf, "Life after charge noise: recent results with transmon

qubits," *Quantum Information Processing*, vol. 8, pp. 105–115, 2008. [Online]. Available: https://api.semanticscholar.org/CorpusID:27305073

[18] D. Reilly, "Challenges in scaling-up the control interface of a quantum computer," 12 2019, pp. 31.7.1–31.7.6.

[19] S. Krinner, S. Storz, P. Kurpiers, P. Magnard, J. Heinsoo, R. Keller, J. Lütolf, C. Eichler, and A. Wallraff, "Engineering cryogenic setups for 100-qubit scale superconducting circuit systems," *EPJ Quantum Technology*, vol. 6, no. 1, p. 2, May 2019. [Online]. Available: https://doi.org/10.1140/epjqt/s40507-019-0072-0

[20] P. Campagne-Ibarcq, P. Six, L. Bretheau, A. Sarlette, M. Mirrahimi, P. Rouchon, and B. Huard, "Observing quantum state diffusion by heterodyne detection of fluorescence," *Phys. Rev. X*, vol. 6, p. 011002, Jan 2016. [Online]. Available: https://link.aps.org/doi/10.1103/PhysRevX.6.011002

[21] N. Wu, J. Lin, C. Xie, Z. Guo, W. Huang, L. Zhang, Y. Zhou, X. Sun, J. Zhang, W. Guo, X. Linpeng, S. Liu, Y. Liu, W. Ren, Z. Tao, J. Jiang, J. Chu, J. Niu, Y. Zhong, and D. Yu, "In situ mixer calibration for superconducting quantum circuits," *Applied Physics Letters*, vol. 125, no. 20, p. 204003, 11 2024. [Online]. Available: https://doi.org/10.1063/5.0234579

[22] S. W. Jolin, R. Borgani, M. O. Tholén, D. Forchheimer, and D. B. Haviland, "Calibration of mixer amplitude and phase imbalance in superconducting circuits," *Review of Scientific Instruments*, vol. 91, no. 12, p. 124707, 12 2020. [Online]. Available: https://doi.org/10.1063/5.0025836

[23] S. Felicetti, D. Z. Rossatto, E. Rico, E. Solano, and P. Forn-D'iaz, "Two-photon quantum rabi model with superconducting circuits," *Physical Review A*, vol. 97, p. 013851, 2017. [Online]. Available: https://api.semanticscholar.org/CorpusID:119370853

[24] E. Jaynes and F. Cummings, "Comparison of quantum and semiclassical radiation theories with application to the beam maser," *Proceedings of the IEEE*, vol. 51, no. 1, pp. 89–109, 1963.

[25] R. Bianchetti, S. Filipp, M. Baur, J. M. Fink, M. Göppl, P. J. Leek, L. Steffen, A. Blais, and A. Wallraff, "Dynamics of dispersive single-qubit readout in circuit quantum electrodynamics," *Phys. Rev. A*, vol. 80, p. 043840, Oct 2009. [Online]. Available: https://link.aps.org/doi/10.1103/PhysRevA.80.043840

[26] D. D. Bernardis, A. Mercurio, and S. D. Liberato, "Tutorial on nonperturbative cavity quantum electrodynamics: is the jaynes–cummings model still relevant?" *J. Opt. Soc. Am. B*, vol. 41, no. 8, pp. C206–C221, Aug 2024. [Online]. Available: https://opg.optica.org/josab/abstract.cfm?URI=josab-41-8-C206

[27] C. P. Koch, U. Boscain, T. Calarco, G. Dirr, S. Filipp, S. J. Glaser, R. Kosloff, S. Montangero, T. Schulte-Herbrüggen, D. Sugny, and F. K. Wilhelm, "Quantum optimal control in quantum technologies. strategic report on current status, visions and goals for research in europe," *EPJ Quantum Technology*, vol. 9, no. 1, p. 19, Jul 2022. [Online]. Available: https://doi.org/10.1140/epjqt/s40507-022-00138-x

[28] C. T. Rigetti and M. H. Devoret, "Fully microwave-tunable universal gates in superconducting qubits with linear couplings and fixed transition frequencies," *Physical Review B*, vol. 81, p. 134507, 2010. [Online]. Available: https://api.semanticscholar.org/CorpusID:35309116

[29] M. F. Russ, S. G. J. Philips, X. Xue, and L. M. K. Vandersypen, "Simple framework for systematic high-fidelity gate operations," *Quantum Science and Technology*, vol. 8, no. 4, 2023. [Online]. Available: https://doi.org/10.1088/2058-9565/acf786

[30] Z. Fillingham, H. Nevisi, and S. Dora, "Optimisation of pulse waveforms for qubit gates using deep learning," 2024. [Online]. Available: https://arxiv.org/abs/2408.02376

[31] G. Lindblad, "On the generators of quantum dynamical semigroups," *Communications in Mathematical Physics*, vol. 48, no. 2, pp. 119–130, Jun 1976. [Online]. Available: https://doi.org/10.1007/BF01608499

[32] I. Wolff, "Microwave mixers, second edition, by stephen a. maas, artech house, boston, london 1993. 375 pages, 165 pages, 8 tables, 161 references, index. price: Us $76.00 and £59.00 in europe. isbn 0-98006-605-1," *International Journal of Microwave and Millimeter-Wave Computer-Aided Engineering*, vol. 3, no. 4, pp. 471–471, 1993. [Online]. Available: https://onlinelibrary.wiley.com/doi/abs/10.1002/mmce.4570030421

[33] J. Clarke and F. K. Wilhelm, "Superconducting quantum bits," *Nature*, vol. 453, no. 7198, pp. 1031–1042, Jun 2008. [Online]. Available: https://doi.org/10.1038/nature07128

[34] H. D. Menendez, L. Bello, and D. Clark, "Dynamic output state classification for quantum computers," in *2023 IEEE/ACM 4th International Workshop on Quantum Software Engineering (Q-SE)*, 2023, pp. 16–23.

[35] M. J. Peterer, S. J. Bader, X. Jin, F. Yan, A. Kamal, T. J. Gudmundsen, P. J. Leek, T. P. Orlando, W. D. Oliver, and S. Gustavsson, "Coherence and decay of higher energy levels of a superconducting transmon qubit." *Physical review letters*, vol. 114 1, p. 010501, 2014. [Online]. Available: https://api.semanticscholar.org/CorpusID:2763310

[36] H. M. Wiseman, "Quantum trajectories and quantum measurement theory," *Quantum and Semiclassical Optics: Journal of the European Optical Society Part B*, vol. 8, no. 1, p. 205–222, Feb. 1996. [Online]. Available: http://dx.doi.org/10.1088/1355-5111/8/1/015

[37] F. Motzoi, J. M. Gambetta, P. Rebentrost, and F. K. Wilhelm, "Simple pulses for elimination of leakage in weakly nonlinear qubits," *Phys. Rev. Lett.*, vol. 103, p. 110501, Sep 2009. [Online]. Available: https://link.aps.org/doi/10.1103/PhysRevLett.103.110501

[38] L. S. Theis, F. Motzoi, F. K. Wilhelm, and M. Saffman, "High-fidelity rydberg-blockade entangling gate using shaped, analytic pulses," *Phys. Rev. A*, vol. 94, p. 032306, Sep 2016. [Online]. Available: https://link.aps.org/doi/10.1103/PhysRevA.94.032306

[39] A. P. Peirce, M. A. Dahleh, and H. Rabitz, "Optimal control of quantum-mechanical systems: Existence, numerical approximation, and applications," *Phys. Rev. A*, vol. 37, pp. 4950–4964, Jun 1988. [Online]. Available: https://link.aps.org/doi/10.1103/PhysRevA.37.4950

[40] N. Khaneja, T. Reiss, C. Kehlet, T. Schulte-Herbrüggen, and S. J. Glaser, "Optimal control of coupled spin dynamics: design of nmr pulse sequences by gradient ascent algorithms," *Journal of Magnetic Resonance*, vol. 172, no. 2, pp. 296–305, 2005. [Online]. Available: https://www.sciencedirect.com/science/article/pii/S1090780704003696

[41] E. Genois, N. J. Stevenson, N. Goss, I. Siddiqi, and A. Blais, "Quantum optimal control of superconducting qubits based on machine-learning characterization," 2024. [Online]. Available: https://arxiv.org/abs/2410.22603

[42] Z. An and D. L. Zhou, "Deep reinforcement learning for quantum gate control," *EPL (Europhysics Letters)*, vol. 126, no. 6, p. 60002, Jul. 2019. [Online]. Available: http://dx.doi.org/10.1209/0295-5075/126/60002

[43] T. Fösel, P. Tighineanu, T. Weiss, and F. Marquardt, "Reinforcement learning with neural networks for quantum feedback," *Phys. Rev. X*, vol. 8, p. 031084, Sep 2018. [Online]. Available: https://link.aps.org/doi/10.1103/PhysRevX.8.031084

[44] M. Bukov, A. G. R. Day, D. Sels, P. Weinberg, A. Polkovnikov, and P. Mehta, "Reinforcement learning in different phases of quantum control," *Phys. Rev. X*, vol. 8, p. 031086, Sep 2018. [Online]. Available: https://link.aps.org/doi/10.1103/PhysRevX.8.031086

[45] L. Viola and S. Lloyd, "Dynamical suppression of decoherence in two-state quantum systems," *Phys. Rev. A*, vol. 58, pp. 2733–2744, Oct 1998. [Online]. Available: https://link.aps.org/doi/10.1103/PhysRevA.58.2733

[46] G. de Lange, Z. H. Wang, D. Ristè, V. V. Dobrovitski, and R. Hanson, "Universal dynamical decoupling of a single solid-state spin from a spin bath," *Science*, vol. 330, no. 6000, pp. 60–63, 2010. [Online]. Available: https://www.science.org/doi/abs/10.1126/science.1192739

[47] K. Khodjasteh and D. A. Lidar, "Fault-tolerant quantum dynamical decoupling," *Phys. Rev. Lett.*, vol. 95, p. 180501, Oct 2005. [Online]. Available: https://link.aps.org/doi/10.1103/PhysRevLett.95.180501

[48] J. Zhang and D. Suter, "Experimental protection of two-qubit quantum gates against environmental noise by dynamical decoupling," *Phys. Rev. Lett.*, vol. 115, p. 110502, Sep 2015. [Online]. Available: https://link.aps.org/doi/10.1103/PhysRevLett.115.110502

[49] J. Braumüller, L. Ding, A. P. Vepsäläinen, Y. Sung, M. Kjaergaard, T. Menke, R. Winik, D. Kim, B. M. Niedzielski, A. Melville, J. L. Yoder, C. F. Hirjibehedin, T. P. Orlando, S. Gustavsson, and W. D. Oliver, "Characterizing and optimizing qubit coherence based on squid geometry," *Phys. Rev. Appl.*, vol. 13, p. 054079, May 2020. [Online]. Available: https://link.aps.org/doi/10.1103/PhysRevApplied.13.054079

[50] M. W. Johnson, P. Bunyk, F. Maibaum, E. Tolkacheva, A. J. Berkley, E. M. Chapple, R. Harris, J. Johansson, T. Lanting, I. Perminov, E. Ladizinsky, T. Oh, and G. Rose, "A scalable control system for a superconducting adiabatic quantum optimization processor," *Superconductor Science and Technology*, vol. 23, no. 6, p. 065004, Apr. 2010. [Online]. Available: http://dx.doi.org/10.1088/0953-2048/23/6/065004

[51] M. O. Tholén, R. Borgani, G. R. Di Carlo, A. Bengtsson, C. Križan, M. Kudra, G. Tancredi, J. Bylander, P. Delsing, S. Gasparinetti, and D. B. Haviland, "Measurement and control of a superconducting quantum processor with a fully integrated radio-frequency system on a chip," *Review of Scientific Instruments*, vol. 93, no. 10, p. 104711, 10 2022. [Online]. Available: https://doi.org/10.1063/5.0101398

[52] Y. Xu, G. Huang, J. Balewski, R. Naik, A. Morvan, B. Mitchell, K. Nowrouzi, D. Santiago, and I. Siddiqi, "Qubic: An open-source fpga-based control and measurement system for superconducting quantum information processors," *IEEE Transactions on Quantum Engineering*, vol. PP, pp. 1–1, 09 2021.

[53] R. Carobene, A. Candido, J. Serrano, A. Orgaz-Fuertes, A. Giachero, and S. Carrazza, "¡tt¿qibosoq¡/tt¿: an open-source framework for quantum circuit rfsoc programming," *Quantum Science and Technology*, vol. 10, no. 3, p. 035010, Apr. 2025. [Online]. Available: http://dx.doi.org/10.1088/2058-9565/adcd97